Forced light scattering by broad-bandwidth incoherent pump lasers

A. Kummrow, S. Woggon, and A. Lau
Max-Born-Institut für Nichtlineare Optik und Kurzzeitspektroskopie im Forschungsverbund, Berlin e.V., Rudower Chaussee 6, D-12474 Berlin, Germany
(Received 21 April 1994; revised manuscript received 19 July 1994)

Forced light scattering using broad-bandwidth incoherent pump light ($\lambda_B = 508$ nm, full width at half maximum $\Delta\lambda_B = 13.8$ nm), and narrow-bandwidth probe light is investigated experimentally and compared with self-diffraction. Forced light scattering improves the dynamic range of measurement by an order of magnitude compared to self-diffraction. A theoretical analysis of this scheme is presented. The technique is used to measure the dephasing kinetics of solutions of crystal violet and bis-(dimethylamino)heptamethine. Resulting from the relatively large autocorrelation time of 40 fs, the experimental signals show no influence from inhomogeneous broadening of the absorption bands; the dephasing kinetics can be characterized by a dephasing time $T_2 \approx 10$ fs and an intrinsic correlation time $\tau_C \approx 30$ fs with a weak modulation (center frequencies ranging from 800 to 1200 cm^{-1}), which is attributed to a coherent motion of the molecule (vibration). The dephasing kinetics of crystal violet shows a close agreement with the dephasing kinetics of malachite green previously reported for two-pulse photon echoes with ultrashort pulses [P. C. Becker *et al.*, Phys. Rev. Lett. **63**, 505 (1989)].

PACS number(s): 42.65.Re

I. INTRODUCTION AND SURVEY OF PREVIOUS WORK

Optical dephasing experiments can be applied to study static and dynamic properties of condensed matter, e.g., semiconductors or dye molecules dissolved in solution. For vibrational transitions in molecules, dephasing occurs within a time ranging from 100 fs up to a few picoseconds, as found using time-resolved coherent Stokes or anti-Stokes scattering. By contrast, the optical dephasing of electronic transitions develops more rapidly at room temperature. Recently developed laser systems allow one to generate pulses of well below 100-fs duration [1–8]. Using such pulses the dephasing of electronic transitions can be monitored in real time. Prior to 1986 pulses of approximately 70-fs duration were used to investigate dye molecules (e.g., Nile blue and cresyl violet) in solution and polymer host [9–12]. The results of these experiments are explicable in terms of a predominantly homogeneous broadening at room temperature with a dephasing time ≤ 20 fs.

The experiments were repeated subsequently using shorter laser pulses with duration ≤ 10 fs providing some insight into the details of the dephasing kinetics. In photon echo experiments using such pulses, deviations from the dephasing of a homogeneous broadened line were observed in several different respects [13–19]. One deviation is a nonmonotonic decay of the coherence peak. Oscillations were found on the decay of the coherence peak for Nile blue and malachite green, which can be related to vibrational modes of the dye molecule [13,16,17]. In addition, the signal peak does not appear at zero delay for Nile blue, LD690, and cresyl violet [13,18]. However it should be noted that the peaks appear at zero delay for malachite green and resorufin [13,14], so that peaking at nonzero delay could probably be a speciality of the oxazonium dyes. Finally an asymmetric form of the coherence peak was found for Nile blue, malachite green, and resorufin, but not for cresyl violet [13–16,18,19].

Though not all of the deviations are found for all dyes, the consideration of models not only assuming simple homogeneous broadening is obviously in order for experiments using pulses of ~ 10 fs duration. The experimental data obtained on this time scale can widely be explained by the optical analog of the Kubo model [20–25]. For a description of details of the non-Markovian dephasing, the more advanced multimode Brownian oscillator model was introduced [14,15,19].

In this paper we propose the application of a method (see *Note added.*) to study the dephasing of electronic transitions, which applies incoherent light instead of femtosecond pulses. Ten years ago, groups in Japan and America recognized independently that the experimental time resolution is given by the correlation time of the laser light and not by the pulse duration [26–29]. This means that pulses with femtosecond duration are not necessarily needed; only femtosecond correlation time is required. Such a short correlation time can be realized quite easily with a non-transform-limited broadband dye laser. The desired laser wavelength is obtained by choosing a suitable laser dye.

A fundamental drawback of all degenerate four-wave mixing experiments is that the stray light from the sample limits the dynamic range of measurement. In principle the stray light can be reduced by spatial filtering, but this reduces the signal level as well.

The scheme of forced light scattering to study ultrafast dephasing processes in large molecules, presented here, uses incoherent pulses generated in a broadband dye laser to generate a phase grating in the sample from which a coherent laser beam at a different frequency is scattered to determine the phase relaxation kinetics. The frequency ω_N of this third beam is chosen in the transparent re-

gion of the dye solution, so that the signal is not partially absorbed as in the self-diffraction scheme. In addition, the intensity of the probing beam can be much higher than the intensity of the pump beams, since the probe laser frequency is not in one-photon resonance and does not change the population of the electronic levels. A third advantage is that the direction of the probing beam can be phase matched. The self-diffraction is possible only for optical thin gratings [30,31].

In Secs. II and III we present experimental results for two dyes in solution showing that the dynamic range of forced light scattering exceeds that of self-diffraction by one order of magnitude, resulting in highly reliable and accurate information on phase relaxation. Within the experimental accuracy, the data are consistent with results form comparative self-diffraction experiments. Section IV gives a theoretical analysis of forced light scattering by incoherent pump beams with scanned delay time. Our experiments use incoherent light with an autocorrelation time of 40 fs. On this time scale, only small deviations from homogeneous dephasing are expected in view of previous experiments with ultrashort pulses of comparable duration. A general approach to more complicated dephasing kinetics will be considered in Sec. IV, since our method is in principle not limited in resolving these processes. Merely incoherent broadband lasers with a higher bandwidth have to be developed for this purpose. Section V is devoted to the discussion of the experimental results. The dephasing kinetics obtained for crystal violet will be compared with real time photon echo experiments on malachite green previously reported by Becker *et al.* [13]. Potential surface parameters previously determined by resonance coherent anti-Stokes Raman scattering (CARS) are used to analyze the results for the heptamethine dye.

II. EXPERIMENTAL METHOD

The broadband laser was a coumarin 152a dye laser transversely pumped at 355 nm with the third harmonic of a Q-switched Nd:YAG laser (where YAG denotes yttrium aluminum garnet, t_p is 6 ns, and the pump energy is 10 mJ). The laser had a 10-cm-long hemispherical resonator with an aluminium-coated concave mirror and an uncoated flat glass window as output coupler. Spectral line narrowing in the course of a nanosecond pulse was avoided using an output coupler with a low reflectance of only 4%. The shot to shot stability of the laser spectrum shown in Fig. 1 was checked with an optical multichannel analyzer. The pulse duration amounted to 3 ns. The output of the broadband laser was passed through a polarizer to obtain a linearly polarized excitation for the scattering experiment.

The theoretical analysis of the experiment is easier if the probing laser has a small linewidth because the dynamic properties of a narrow-band laser can be ignored then. The narrow-band laser light of the probe beam was generated with tunable dye lasers using a standard grazing incidence arrangement, which gave a linewidth below 1 cm^{-1}. We used a coumarin 153 dye laser pumped at 355 nm to obtain narrow-band laser light at

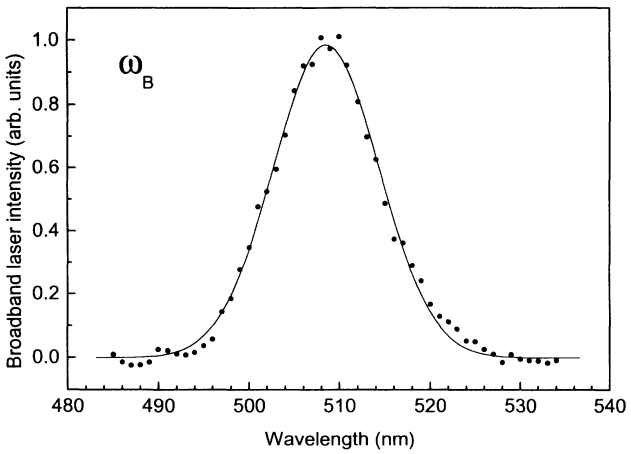

FIG. 1. Broadband laser spectrum. The experimental points are fitted with a Gaussian distribution centered at $\lambda_B = 508$ nm and a FWHM of $\Delta\lambda_B = 13.8$ nm.

550 nm for experiments with heptamethine molecules. A DCM (4-dicyanomethylene-2-methyl-6-(*p*-dimethylaminostyryl)-4*H*-pyran) dye laser pumped at 532 nm was applied in experiments with crystal violet. The DCM laser was operated at 650 nm, so that the probe light is always outside the absorption band of the investigated dye. The term *O-O* transition is used here for the optical transition from the lowest vibrational level in the ground state to the lowest vibrational level in the electronically excited state.

The broadband beam was split in a Michelson interferometer with scanned delay time (step width 6.7 fs). Using an objective with 100-mm focal length, the two broadband laser beams and the narrow-band laser beam were overlapped. The focus size in the sample cuvette was 100 μm and the thickness of the cuvette amounted to 200 μm. The energy per beam was typically 15 μJ.

The beams were arranged in a folded box arrangement as sketched in Fig. 2. The broadband beams with direction $\mathbf{k}_1$ and $\mathbf{k}_2$ form the light grating with grating vector

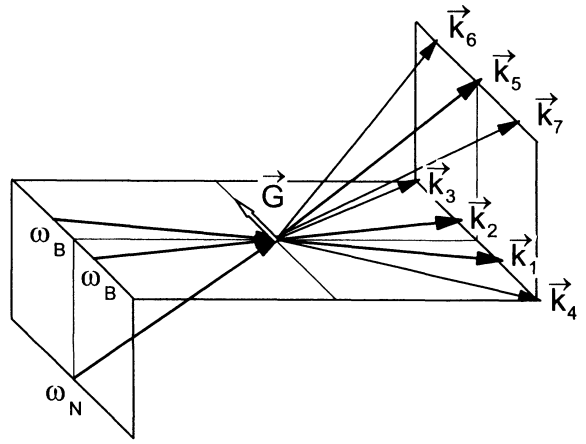

FIG. 2. $\mathbf{k}_1$ and $\mathbf{k}_2$, broadband pump beams (frequency ω_B); $\mathbf{k}_5$, narrow-band probe beam (frequency ω_N); $\mathbf{k}_{3,4}$, self-diffraction signals (photon echo); $\mathbf{k}_{6,7}$, forced light scattering signals (stimulated photon echo).

$\mathbf{G}=\mathbf{k}_2-\mathbf{k}_1$. The beams with directions $\mathbf{k}_3=\mathbf{k}_2+\mathbf{G}$ and $\mathbf{k}_4=\mathbf{k}_1-\mathbf{G}$ are generated by self-diffraction. In these directions the photon echoes are emitted if the electronic transition of the sample is inhomogeneously broadened. The probe light (direction $\mathbf{k}_5$) is partially diffracted into the directions $\mathbf{k}_{6,7}=\mathbf{k}_5\pm\mathbf{G}$. The signals in the directions $\mathbf{k}_3$, $\mathbf{k}_4$, $\mathbf{k}_6$, and $\mathbf{k}_7$ were detected with photodiodes. They were measured as a function of delay time between beam 1 and beam 2.

A comment should be made on stimulated photon echoes emitted into the directions $\mathbf{k}_6$ and $\mathbf{k}_7$, which have been observed in experiments with ultrashort pulses [9,16,18]. In our scheme, no such stimulated photon echoes can be expected because the probe beam can be viewed as a quasicontinuous wave. The forced light scattering of the probe laser is basically a $\chi^{(1)}$ process. It is the diffraction by a phase grating, which is induced by the incoherent pump laser beams. For nonzero delay time between the two pump beams, the amplitude of the phase grating is reduced compared to zero delay time. So the dephasing of the electronic transition is indirectly monitored by forced light scattering. A qualitative analysis will be presented in Sec. IV.

III. EXPERIMENTAL RESULTS

We investigated the electronic dephasing kinetics of a polymethine dye and of crystal violet, a triphenyl methane dye. Polymethine dyes are known for a long time as sensitizers in silver-based photography. In recent

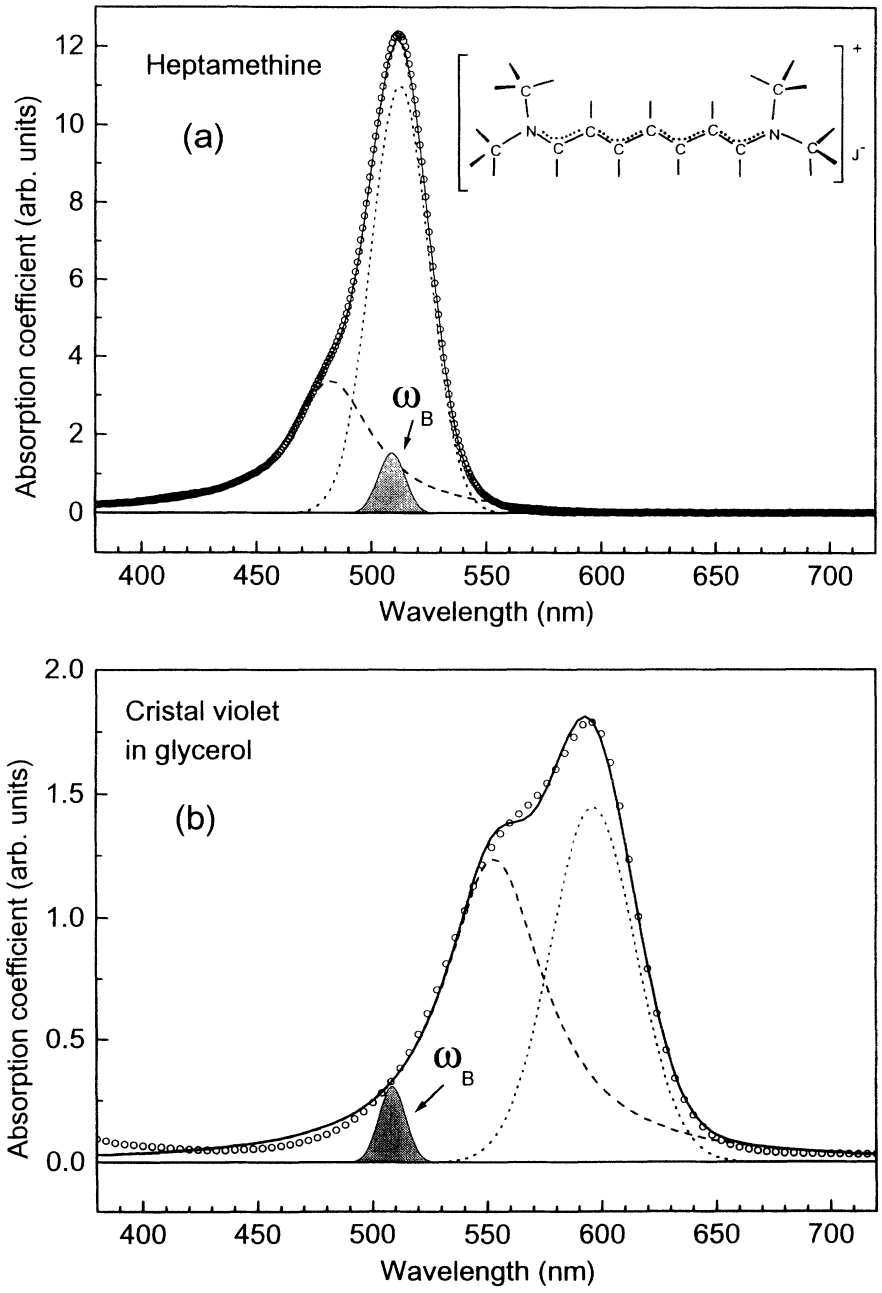

FIG. 3. Linear absorption spectra of the three dye solutions (always 1×10^{-3} mol/l). The heuristic fit (solid line) uses a Lorentzian line shape (broken line) for the short-wavelength side and a Gaussian (dotted line) for the long-wavelength side: (a) bis-(dimethylamino) heptamethine iodide in ethanol; (b) crystal violet chloride in glycerol; (c) crystal violet chloride in water. The broadband laser spectrum ω_B is shown as the hatched area.

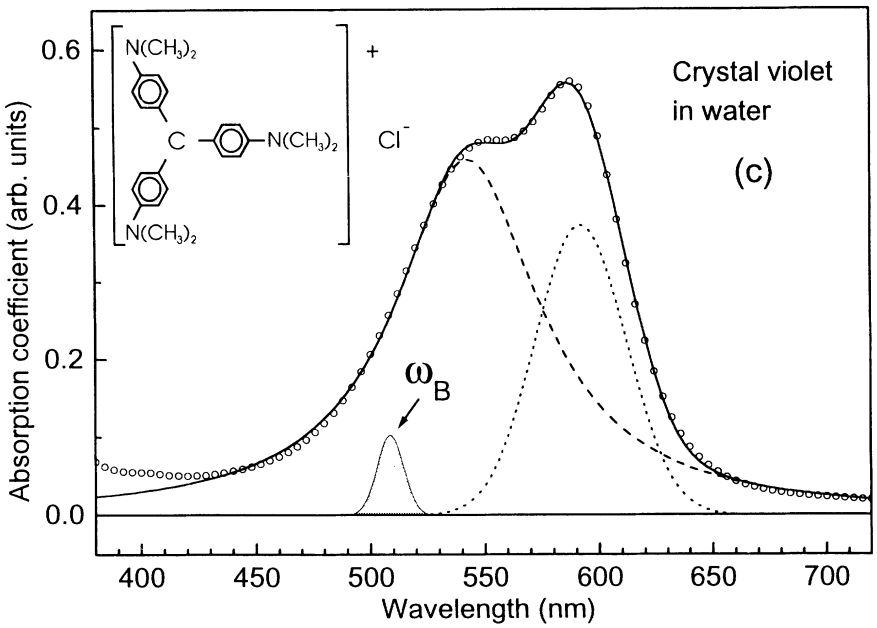

FIG. 3. (*Continued*).

years methine dyes have received growing interest as model molecules for studying the correlation between structure and nonlinear parameters [32]. They show the highest contribution to the third-order hyperpolarizabilities per single π electron found within one-dimensional organic structures, as a result of the perfect bond order equalization along the methine chain. Figure 3(a) shows the absorption spectra of the dye solutions used in the experiment. The broadband dye-laser frequency fits to the 0-0 transition of the heptamethine dye. The term 0-0 transition is used here for the optical transition from the lowest vibrational level in the ground state to the lowest vibrational level in the electronically excited state.

For comparison, we investigate solutions of crystal violet chloride. This dye is excited far above the 0-0 transition [Figs. 3(b) and 3(c)]. It is well known that the ground-state recovery time of crystal violet can be modified significantly by changing the solvent viscosity [33]. In addition, a viscosity dependence of the dephasing kinetics has already been reported for Nile blue observed in a femtosecond three-pulse photon echo experiment [16]. Therefore, we tried water and glycerol as solvents, which have a viscosity ratio of about 800, to look for an influence on the dephasing process.

Results on the dephasing kinetics for bis-(dimethylamino)heptamethine iodide and for crystal violet are presented in Figs. 4 and 5, respectively. All beams in the scattering experiment are polarized parallel to each other. Significant differences were not found for the dephasing of crystal violet in water and glycerol [Fig. 5(b)]. So no influence from the solvent viscosity is observed. For crossed polarization of the two broadband pump beams the signal for self-diffraction and forced light scattering was reduced, but no change of the delay-time dependence was observed. The results for crossed polarization were not analyzed further because the dynamic range of measurement was only 10^2.

The experimental results are well fitted with a Gaussian curve for delay times $|\tau| < 50$ fs (Figs. 4 and 5). How-

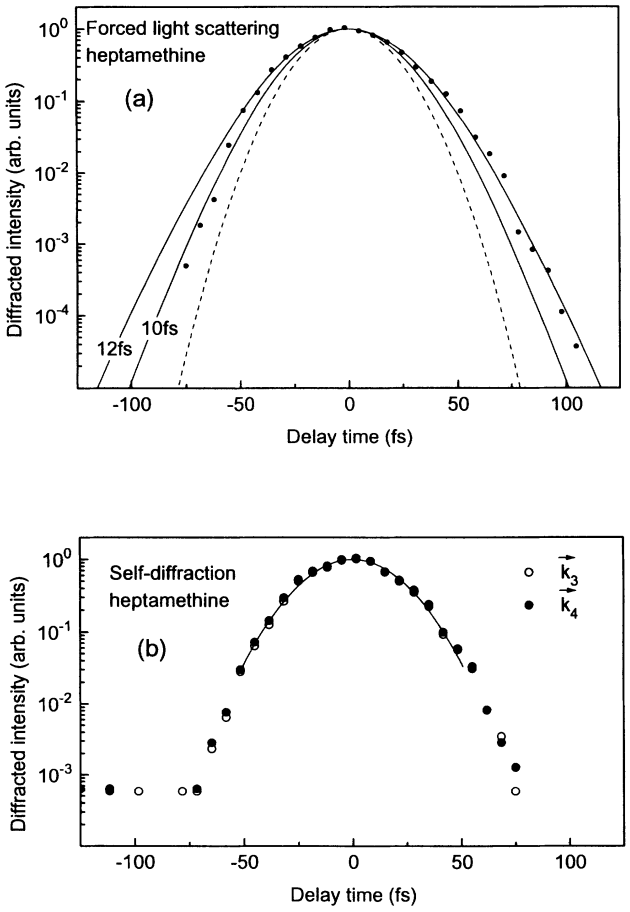

FIG. 4. Diffracted intensity for heptamethine in ethanol (1×10^{-3} mol/l): (a) force light scattering done at 550 nm [solid lines, two fits using $T_2 = 10$ and 12 fs ($\tau_C/T_2 = 3$); broken line, calculated autocorrelation function of the broadband laser]; (b) self-diffraction in the directions $\mathbf{k}_3$ and $\mathbf{k}_4$ (solid line, Gaussian fit for the data points around zero delay).

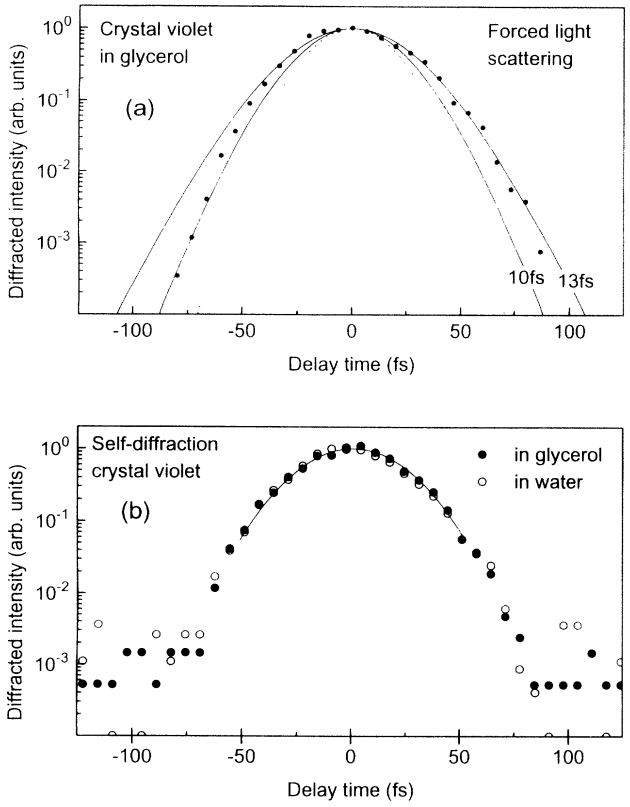

FIG. 5. Diffracted intensity for crystal violet chloride (1×10^{-3} mol/l): (a) forced light scattering done at 650 nm [solvent, glycerol; solid lines, two fits using $T_2=10$ and 13 fs ($\tau_C/T_2=3$); broken line, calculated autocorrelation function of the broadband laser]; (b) self-diffraction for dye dissolved in glycerol and water (solid line, Gaussian fit for the data points around zero delay).

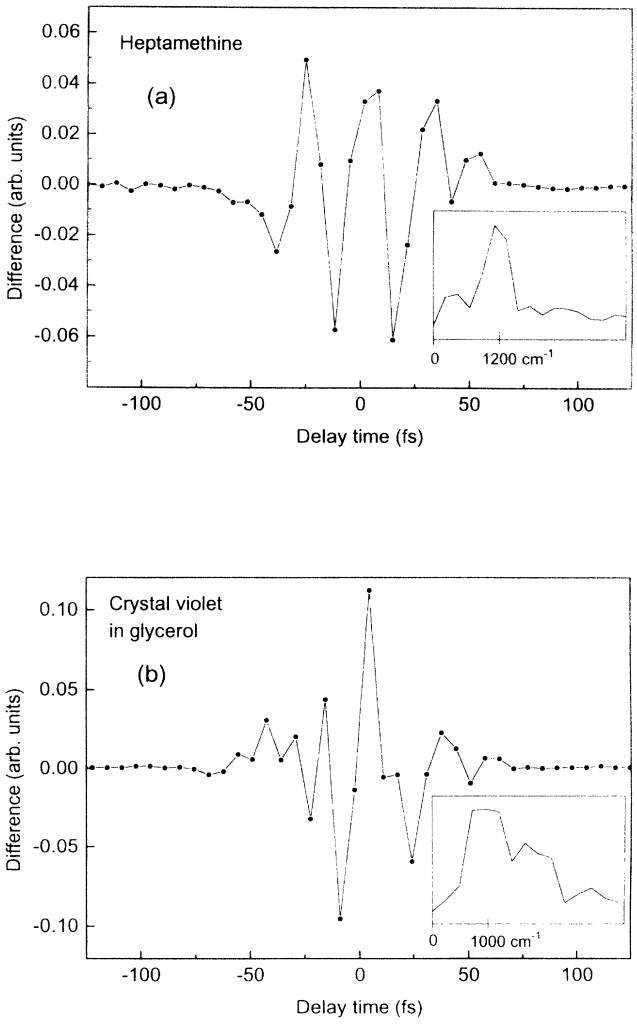

ever, the difference between the least-squares fit and the experimental data points turns out to be a rapidly oscillating function (Fig. 6). The damping is the same as for the Gaussian fit. The oscillation is analyzed using a Fourier transformation of the difference curve. The Fourier amplitudes are shown as insets. The peak in the Fourier spectrum corresponds to the oscillation frequency and is 1200 cm^{-1} for heptamethine in ethanol and 1000 and 800 cm^{-1} for crystal violet in glycerol and water, respectively. The width of the Fourier spectrum is partially caused by the damping of the oscillation.

Figure 4(b) shows that there is no temporal shift between the self-diffracted signals recorded in the $\mathbf{k}_3$ and $\mathbf{k}_4$ directions within our experimental resolution (5 fs). The self-diffraction scheme is very attractive, whenever a temporal shift between signals recorded in the $\mathbf{k}_3$ and $\mathbf{k}_4$ directions can be obtained, which is the case for large inhomogeneous broadening. This is because only a small dynamic range is required to measure T_2 then. The failure to detect such a temporal shift might result from thermal gratings [34], which are frequently encountered for parallel polarization of the pump beams. However, we even observed no splitting for crossed polarization of

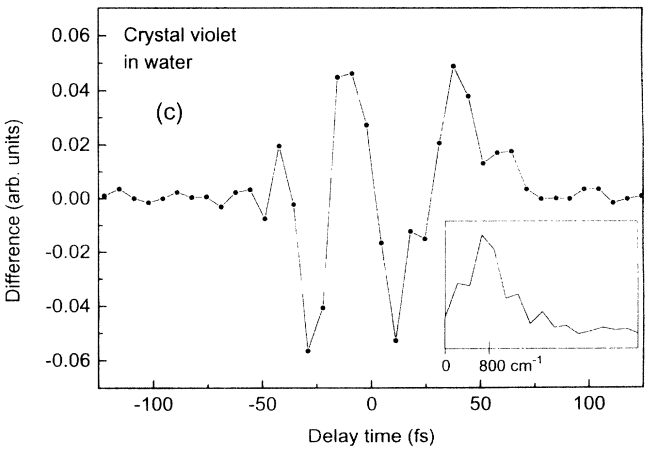

FIG. 6. Difference between experimental data and Gaussian least-squares fit to the three different dye solutions as function of delay time. The damped oscillations are analyzed using Fourier transformation (spectrum shown as the inset); (a) heptamethine in ethanol; (b) crystal violet in glycerol; (c) crystal violet in water

the pump beams. This indicates the absence of a photon-echo-like response and that inhomogeneous broadening is not apparent.

IV. MODEL FOR FORCED LIGHT SCATTERING

A. Coupling between the light field and the molecular system: Bloch equations

We take as our starting point the Bloch equations for an ensemble of two-level systems. The two levels are electronic states of the dye molecule. The broadband incoherent light with frequency ω_B is in resonance with the (individual) transition frequency ω_0 of the two-level system ($\omega_B \cong \omega_0$). The two-level system is also coupled to a thermal bath represented by the solvent. Sometimes it is useful to include those degrees of freedom of the molecule into the thermal bath, which are not coupled directly with the electronic transition (e.g., rotational modes). The motion of the system is described with the density-matrix formalism using Bloch equations:

$$\partial\rho_D/\partial t = -2i(H_{ab}\rho_{ba} - H_{ba}\rho_{ab})/\hbar - (\rho_D - \rho_D^{(0)})/T_1 , \tag{1}$$

$$\partial\rho_{ba}/\partial t = iH_{ba}\rho_D/\hbar - (T_2^{-1} + i\omega_0)\rho_{ba} , \tag{2}$$

$$H_{ba} = H_{ab}^* = -\mu\hat{E}(\mathbf{r},t)\exp(-i\omega_B t) + \text{c.c.} \tag{3}$$

Here ρ_{ba} and ρ_{ab} are the off-diagonal elements of the density matrix and $\rho_D = \rho_{aa} - \rho_{bb}$, μ is the transition dipole moment, and T_1 and T_2 are the longitudinal and transverse relaxation time.

The narrow-band probe light is off resonance. Therefore, the electric light field in (3) contains only contributions from the fluctuating electric fields $\tilde{E}_{1,2}$ of the two broadband laser beams:

$$\hat{E}(\mathbf{r},t) = \tilde{E}_1(\mathbf{r},t)\exp(i\mathbf{k}_1\cdot\mathbf{r}) + \tilde{E}_2(\mathbf{r},t)\exp(i\mathbf{k}_2\cdot\mathbf{r}) . \tag{4}$$

As mentioned at the end of Sec. II, the diffraction of the probe beam is caused by the refractive index change resulting from the change of ρ_D. This change is calculated using the standard second-order perturbation analysis and the rotating-wave approximation. Using the starting condition

$$\rho_{ba}^{(0)} = \rho_{ab}^{(0)*} = 0, \quad \rho_D^{(0)} = \rho_0 , \tag{5}$$

one obtains, similarly to Ref. [28],

$$\rho_D^{(2)}(t) = -\frac{2\mu^2\rho_0}{\hbar^2}\int_{-\infty}^{t} dt_1 \int_{-\infty}^{t_1} dt_2 \exp[-(t-t_1)/T_1]\{\hat{E}(\mathbf{r},t_1)\hat{E}(\mathbf{r},t_2)\exp[-g^*(t_1-t_2)] + \hat{E}^*(\mathbf{r},t_1)\hat{E}(\mathbf{r},t_2)\exp[-g(t_1-t_2)]\} , \tag{6}$$

where $g(t) = (i\Delta + T_2^{-1})t$ and $\Delta = \omega_0 - \omega_B$. Only the second summand in the curly brackets in (6) contributes to the diffraction because only this term is spatially modulated with the grating period [see Eq. (4)]. Taking only the relevant terms in (6) gives ($\mathbf{G} = \mathbf{k}_2 - \mathbf{k}_1$ is the grating vector)

$$\rho_D^{(2)}(t;\mathbf{G}) = -\frac{2\mu^2\rho_0}{\hbar^2}\int_{-\infty}^{t} dt_1 \int_{-\infty}^{t_1} dt_2 [\tilde{E}_1^*(\mathbf{r},t_1)\tilde{E}_2(\mathbf{r},t_2) + \tilde{E}_2^*(\mathbf{r},t_1)\tilde{E}_1(\mathbf{r},t_2)]\exp[-(t-t_1)/T_1 - g(t_1-t_2)] . \tag{7}$$

The two broadband fields are produced by beam splitting and a temporal delay τ for beam 2. Since the two beams are overlapped in the sample under an angle, different spatial locations in the sample see different delays

$$\Delta t = \tau + \mathbf{G}\cdot\mathbf{r}/\omega_B , \tag{8}$$

where $\mathbf{r}$ is measured from the center of the sample. An upper limit for the spatial variant part is $\pi n_G/\omega_B$, where n_G is the number of "lines" of the grating. As we will ignore in the following the spatial variant delay in (8), this limits the time resolution in our experiment [35]. The spatial variant delay is below 5 fs in our experiment and negligible, therefore, compared to the limitation posed by the coherence time of the light (> 10 fs). Thus we use the approximation

$$\tilde{E}_1(\mathbf{r},t) \approx E_B(t)R(t_r+\tau)\exp(-i\omega_B\tau) , \qquad \tilde{E}_2(\mathbf{r},t) \approx E_B(t)R(t_r) , \tag{9}$$

where E_B is the amplitude of the envelope of the broadband laser pulse, t_r is the reduced time

$$t_r = t - (\mathbf{k}_1+\mathbf{k}_2)\cdot\mathbf{r}/2\omega_B , \tag{10}$$

and $R(t)$ is a complex random function describing the incoherence of the broadband laser. The function $E_B(t)$ is a "slowly" varying function of time. The meaning of "slowly" is specified below. To receive results comparable to Ref. [28], we also assume a stationary Gaussian process

$$\langle R^*(t)R(t+\tau)\rangle = D(\tau) , \qquad \langle R(t)R(t+\tau)\rangle = \langle R^*(t)R^*(t+\tau)\rangle = 0 , \qquad \langle R(t)\rangle = \langle R^*(t)\rangle = 0 , \tag{11}$$

where the symbol $\langle\ \rangle$ denotes the statistical average and $D(\tau)$ is the correlation function of the incoherent light. For example, a Gaussian spectral density of the incoherent light results in a correlation function of the form

$$D(\tau) = (\Gamma\sqrt{2\pi})^{-1}\exp[-\tau^2/(2\Gamma^2)] . \tag{12}$$

B. Grating formation

In order to bring out the similarity of forced light scattering by electronic and thermal gratings, we will re-

view briefly the grating formation by interfering incoherent light beams. The absorption changes can be ignored since the narrow-band laser is assumed to be off resonance. The detected signal results predominantly from diffraction by a refractive index grating

$$n(\mathbf{r})=n_0+n_\Delta\cos(\mathbf{G}\cdot\mathbf{r}) . \tag{13}$$

The detected intensity is [36]

$$J_S=T\left[\frac{\pi d}{2\lambda_N}\right]^2 J_N n_\Delta^2 , \tag{14}$$

where T is the sample transmission, d is the sample thickness, and λ_N and J_N are the wavelength and intensity of the probing narrow-band laser.

For crossed polarization of the pump beams, we have a most significant contribution from the change of the linear polarizability of the dye molecule $\Delta\gamma_N^{(1)}$ when going from level a to level b. This "electronic" contribution to the refractive index is also present for parallel polarized pump beams. For the electronic contribution we can write

$$n_\Delta=\Delta\gamma_N^{(1)}Nf(\tau)|E_B(t)|^2 . \tag{15}$$

Here N is the number density of dye molecules and

$$f(\tau)=[\langle\rho_D^{(2)*}(t;\tau)\rho_D^{(2)}(t;\tau)\rangle]^{1/2}/|E_B(t)|^2 . \tag{16}$$

In (16) we took the statistical average because the narrow-band probe laser has no femtosecond time resolution. In other words, the narrow-band laser field E_N must vary slowly compared to the broadband laser fluctuations.

For all beams parallel polarized, as used for the results in Figs. 4 and 5, we have to expect a significant contribution from a thermal grating, which is accumulated over the nanosecond pulse. In order to calculate the thermally induced refractive index change, we determine first the heat production per time and volume

$$q(\mathbf{r},t)=q_0(t)+q_\Delta(t)\cos(\mathbf{G}\cdot\mathbf{r}) . \tag{17}$$

The conversion of the absorbed light into heat proceeds in a two steps: relaxation to the electronic ground state and transfer of energy into the solvent. If the narrow-band laser pulse and the envelope of the broadband laser pulse $[E_B(t)]$ are varying slowly compared to the time needed for thermalization with the solvent bath [37], then we may assume simply that the heat production is in proportion to the pump-laser-induced excited-state population

$$q_\Delta(t)=N\hbar\omega_0 f(\tau)|E_B(t)|^2 . \tag{18}$$

Here we used again the statistical average $f(\tau)$, because the light correlation time (femtosecond time scale) is much shorter than the time for thermalization with the solvent bath (picosecond time scale.

The constant term in (17) is not important for the refractive index modulation, as we will assume that the refractive index n is a linear function of temperature Θ. To calculate the temperature grating amplitude Θ_Δ, we start from the one-dimensional heat flow equation [38]

$$\frac{\partial\Theta}{\partial t}-D_t\frac{\partial^2\Theta}{\partial x^2}=\frac{q(\mathbf{r},t)}{c_V} , \tag{19}$$

where the x direction is parallel to $\mathbf{G}$. D_t is the temperature diffusivity and c_V is the volumetric heat. After spatial Fourier transformation a differential equation for Θ_Δ is obtained [39]

$$d\Theta_\Delta/dt+4\pi^2D_t\Theta_\Delta/\Lambda^2=q_\Delta(t)/c_V \tag{20}$$

(Λ is the grating constant), which is solved by

$$\Theta_\Delta(t)=\frac{1}{c_V}\int_{-\infty}^{t}\exp(-4\pi^2D_t[t-t']/\Lambda^2)q_\Delta(t')dt' . \tag{21}$$

Using (18) in (21) gives, for the thermally induced refractive index modulation,

$$n_\Delta=n_\Theta\Theta_\Delta=f(\tau)\frac{N\hbar\omega_0 n_\Theta}{c_V}\times\int_{-\infty}^{t}|E_B(t')|^2\exp(-4\pi^2D_t[t-t']/\Lambda^2)dt' \tag{22}$$

where n_Θ is the temperature coefficient of the refractive index of the solution. A comparison of (15) with (22) shows that the delay-time dependence is the same for the thermal grating and the electronic grating [namely, $f(\tau)$]. This situation is different for self-diffraction, where the thermal grating leads to a coherence peak as calculated here for the forced light scattering, but the electronic grating gives a different response.

C. Delay-time dependence

The diffracted intensity is proportional to $n_\Delta^2\propto[f(\tau)]^2$ [Eq. (14)]. So the delay-time dependence of the diffracted intensity is governed by this function. From (14) we obtain, for the detected intensity,

$$J_S\propto[f(\tau)]^2=\frac{4\pi^2\mu^4\rho_0^2}{\hbar^4}\int_{-\infty}^{t_r}ds_1\int_{-\infty}^{s_1}ds_2\int_{-\infty}^{t_r}dt_1\int_{-\infty}^{t_1}dt_2[\langle R^*(s_1+\tau)R(s_2)R(t_1+\tau)R^*(t_2)\rangle+\langle R(s_1-\tau)R^*(s_2)R^*(t_1-\tau)R(t_2)\rangle]\times\exp[-(2t_r-s_1-t_1)/T_1-g(t_1-t_2)-g^*(s_1-s_2)] . \tag{23}$$

The fourth-order moments appearing in (23) can be reduced to products of second-order moments if we make the usual assumption of chaotic light [40], e.g.,

$$\langle R^*(s_1+\tau)R(s_2)R(t_1+\tau)R^*(t_2)\rangle=\langle R^*(s_1+\tau)R(s_2)\rangle\langle R^*(t_2)R(t_1+\tau)\rangle+\langle R^*(s_1+\tau)R(t_1+\tau)\rangle\langle R^*(t_2)R(s_2)\rangle$$
$$=D(s_1-s_2+\tau)D(t_1-t_2+\tau)+D(t_1-s_1)D(t_2-s_2)\,, \quad (24)$$

where (11) has been used in the second step. The intensity diffracted into the $\mathbf{k}_6$ and $\mathbf{k}_7$ directions can be calculated analytically for δ-correlated fields [i.e., $D(t)=\delta(t)$, where $\delta(t)$ is the Dirac function]:

$$[f(\tau)]^2=\frac{4\pi^2\mu^4\rho_0^2T_1^2}{\hbar^4}\exp\left[-\frac{2|\tau|}{T_2}\right]. \quad (25)$$

This result can be compared with the results obtained by Morita and Yajima for self-diffraction by electronic gratings [28]. They obtained a rather complicated formula for the intensity diffracted into $\mathbf{k}_3$ direction. The formulas are generally not helpful for an analysis of the self-diffraction signal as a function of delay time. However, in the situation of large population lifetime and negligible inhomogeneous broadening, the intensity decays exponentially with $T_2/2$. The same happens to the signal from forced light scattering.

D. Extension to other dephasing kinetics

In order to go beyond the very simplest dephasing kinetics, different line-shape functions $g(t)$ can be introduced in Eq. (23) [24,25], which describe different relaxation dynamics of the off-diagonal element of the density matrix [Eq. (2)]. For the Bloch model, we used

$$g(t)=i\Delta t=+t/T_2 \quad (26)$$

and for the Kubo model we can take

$$g(t)=i\Delta t+[t-\tau_C+\tau_C\exp(-t/\tau_C)]/T_2\,, \quad (27)$$

where τ_C can be interpreted as the intrinsic correlation time of the fluctuations of the transition frequency of the molecule. An unusual imaginary part appears in the line-shape function (27) because we took $\omega_0\neq\omega_B$ into account.

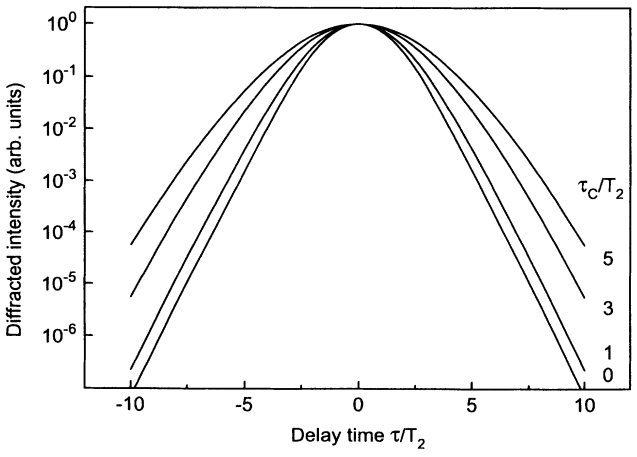

FIG. 7. Calculated diffracted intensity as function of delay time for $\tau_C=0$, T_2, $3T_2$, and $5T_2$ in the Kubo model. The delay time is normalized with respect to the homogeneous dephasing time T_2, which also characterizes the decay for large delay times.

A numerical integration of Eq. (23) is very time consuming because of the fourfold integration. For an interpretation of the dephasing kinetics it suffices to calculate those terms which depend on delay time. According to Eq. (24), there are also terms which do not depend on delay time τ leading to a constant background. This background is zero in the case of Eq. (25), but a nonzero background can arise from nonzero light correlation time or different dephasing kinetics. However, in our experiments, we have no clear evidence of a background caused by coherent coupling, the background is caused by stray light. So we will not determine this constant explicitly. The delay-time dependence can be written as

$$J_S\propto[f(\tau)]^2=\text{const}+\frac{4\pi^2\mu^4\rho_0^2T_1^2}{\hbar^4}\times\left|\int_{-\infty}^{\infty}ds_3D(s_3-\tau)\exp[-g(|s_3|)]\right|^2. \quad (28)$$

Thus, apart from an optional constant background, the delay-time dependence of the diffracted intensity is the absolute square of the convolution of the light correlation function with the dephasing kinetics. Equation (25) is a good example for this relation.

For a delay time $\tau\gg\tau_C+\Gamma$, Eq. (23) gives the same result for both line-shape functions (26) and (27). However, in this case we have to expect $\tau\gg T_2$, which implies that the diffracted signal could be very small. Therefore, numerical examples will be presented here to elucidate the effect of finite correlation time of the molecular transition frequency and of the light field.

In the following we take T_2 as a time unit. Figure 7 shows an example of the diffracted intensity as function of delay time assuming the Kubo model and $\Gamma=1.4T_2$, which corresponds to our experimental situation. For resorufin dissolved in dimethylsulfoxide $\tau_C=2.3T_2$ has been obtained [14]. In Fig. 7, we chose τ_C between 0 (Bloch model) and $5T_2$. For a relate diffracted intensity $<10^{-2}$, all curves show nearly the same exponential decay with $\exp(-2|\tau|/T_2)$, demonstrating that the effect of the nonzero intrinsic correlation time on the dephasing rate is negligible in this region. However, the width of the coherence peak depends strongly on τ_C. Hence T_2 and τ_C can both be derived from the coherence peak, provided the dynamic range of measurement is large enough.

V. DISCUSSION

The absence of a photon-echo-like response in our self-diffraction experiment seems surprising since it is

known, for example, that the absorption band of crystal violet is inhomogeneously broadened [41,42]. Effects from inhomogeneous broadening (or non-Markovian dynamics) were also not found for dye solutions at room temperature in several previous experiments with incoherent light [34,43–45]; photon echoes were reported only for rhodamine B in viscous solvents [46]. Therefore, one might argue that this results from a principle limitation of the incoherent light technique. This would be the case if the time resolution of the incoherent light experiment is lower than the time constant for spectral cross relaxation τ_X since for delay times τ exceeding τ_X the spectral diffusion has scrambled the memory of the original polarization. Ishikawa and Maruyama [42] reported $\tau_X = 0.5$ ps for crystal violet (in methanol). In our experiments we used only delay times below 0.1 ps. Therefore, $\tau_X \gg \tau$ for crystal violet and spectral diffusion plays no role in our experiment.

Despite $\tau_X \gg 100$ fs, an inhomogeneous broadening was not observed directly. This has to be expected, simply because the linewidth of the broadband laser is not larger than the homogeneous broadening of the transition: The broadband pump laser excites only a nearly homogeneous subgroup of the total ensemble of two-level systems since the light correlation time is larger than the dephasing time constant (this is why we are forced to measure in the wings of the coherence peak to resolve the dephasing kinetics). In fact, the experiments with ultrashort pulses of 70-fs duration can also be interpreted in this way (pulse duration larger than dephasing time constant). In order for inhomogeneous broadening of the absorption band to become apparent in the dephasing kinetics, a larger laser linewidth is required.

Unfortunately, the spectral cross relaxation time for the hepamethine dye has not been measured yet. Joo and Albrecht [18] measured $\tau_X = 2.5$ ps for cresyl violet and LD690 (in ethylene glycol) in a three-pulse photon echo experiment. On the other hand, $\tau_X \approx 0.2$ ps was estimated by Bardeen and Shank [17] for Nile blue and LD690 from a very similar experiment. Thus far, there is no simple interpretation for the discrepancy between the two experiments with LD690. So $\tau_X \approx 1$ ps might be a reasonable assumption for dyes in solution at room temperature nevertheless. In the following we will assume that $\tau_X \gg 100$ fs for the heptamethine dye.

The foregoing theoretical treatment showed that the dephasing kinetics can be monitored only if the delay time exceeds the correlation time of the light fields. According to the Wiener-Khintchine theorem [47,48], the autocorrelation function of the broadband laser fields can be calculated from the power spectrum $I_B(\omega)$ of the broadband laser:

$$\langle R^*(t)R(t+\tau)\rangle \propto \int_0^\infty I_B(\omega)\exp[-i(\omega-\omega_B)\tau]d\omega \tag{29}$$

(see also [49]). In our experiments the power spectrum is Gaussian (Fig. 1). Thus the autocorrelation (29) is also a Gaussian function. If $\Delta\lambda_B$ is the full width at half maximum (FWHM) of the power spectrum, then the FWHM $\Delta\tau_B$ of the autocorrelation function is

$$\Delta\tau_B = 0.62\lambda_B^2/(c\Delta\lambda_B) = 2.36\Gamma\ , \tag{30}$$

which is the same as for transform limited Gaussian pulses [50] (note the autocorrelation function is broader by a factor of $\sqrt{2}$ compared to the duration of Gaussian pulses).

For the data given in Fig. 1, $\Delta\tau_B = 39$ fs. The corresponding autocorrelation function is plotted in Fig. 4(a). The detected signal is much larger than the correspondingly normalized autocorrelation of the light for delay times $|\tau| \geq 50$ fs. A decay of the diffracted intensity as function of delay time should be analyzed preferably in this region to determine the dephasing kinetics, so that the required dynamic range of measurement must be very much higher than 10^2. Therefore, forced light scattering is better suited than self-diffraction because we obtained a dynamic range that is ten times higher.

As for ultrashort pulse experiments, the high dynamic range can be used only if spectral cross relaxation plays no role. If spectral cross relaxation poses a limit in the range of < 100 fs, than incoherent light with a shorter correlation time should be applied. However, we expect much larger spectral cross relaxation times, so that we can take full advantage of the improved dynamic range.

A. Hepamethine dye

We will analyze the diffracted intensity as function of delay time assuming "homogeneous" broadening, but allowing for a nonexponential decay according to the Kubo model. The diffracted intensity in Fig. 4(a) decays exponentially for $|\tau| \leq 50$ fs with a decay time 6 ± 1 fs. The experimental curve is too broad for $\tau_C = 0$. The two fit curves in Fig. 4(a) assume $\Delta = 0$, $\tau_C/T_2 = 3$, and $T_2 = 10$ or 12 fs, respectively. The exponential decay time is somewhat larger than $T_2/2$ as a result of $\tau_C \neq 0$. The nonzero τ_C indicate that the underlying stochastic bath process is not in its fast modulation limit [18,25]. From the experimental data, we deduce a dephasing time parameter of $T_2 = 10\pm2$ fs for bis-(dimethylamino) heptamethine and an intrinsic correlation time of $\tau_C \approx 30$ fs. Since the T_1 time of the S_1 state of heptamethine is about 30 ps [51], the self-diffraction intensity should also decay with twice the T_2 time for large decay time, as mentioned at the end of Sec. IV C. Figure 4(b) shows that this is the case.

The absorption spectrum of heptamethine can be modeled assuming contributions from several vibrations and an equal homogeneous broadening for each of the vibrations [52]. The six relevant vibrations (253 and 1300 cm^{-1} being the strongest) have been determined by resonance CARS and spontaneous resonance Raman scattering [52,53]. The resonance CARS experiments gave a homogeneously broadening Γ_{el} in the range of 200–400 cm^{-1} for the vibrations coupled to the electronic transition [53]. The absorption line can be modeled with a homogeneous linewidth of 400 or 600 cm^{-1} for all vibrations, depending on the relative contribution of the different vibrations [52]. Kircheva *et al.* [52] made no attempt to fit the wings of the absorption spectrum, so that an effect of nonzero τ_C could not be resolved. A

linewidth of $\Gamma_{el}=400$ cm^{-1} corresponds to a relaxation time $T_{el}=(2\pi c\Gamma_{el})^{-1}=13$ fs. Since only a part of the absorption band of the heptamethine dye is optically excited, we probably excite only one of the six vibrations efficiently, so that we can expect a homogeneous dephasing with 13 fs. A coherent excitation of additional vibrations will not change the homogeneous dephasing time. Indeed, the 13 fs time agrees quite well with our $T_2=10\pm2$ fs.

The excitation of a dominant vibration and the weak excitation of a further vibration could also explain the residual oscillation on the coherence peak [Fig. 6(a)]. Such an oscillation is usually attributed to a coherent motion of the molecule [13,16,43,44]. This explanation can also be applied here since the oscillation frequency observed in Fig. 6(a) agrees with the beat frequencies of the strongest vibrational modes. In addition it is known from resonance CARS that several vibrations between 1000 and 1400 cm^{-1} are efficiently excited by pump light around 510 nm [54,55].

A modulation of the coherence peak can also result if the absorption is nonuniform over the broadband laser spectrum. Selected absorption for parts of the broadband laser spectrum leads to holes in the power spectrum, as the light penetrates into the dye solution. This causes oscillations in the coherence peak as seen from Eq. (29) (see also [45]). This effect is negligible here because we excited heptamethine only 120 cm^{-1} above the 0-0 transition [Fig. 3(a)], so that the absorption is spectrally constant.

B. Crystal violet

For crystal violet in glycerol the wings of the coherence peak are fitted with a decay rate of 6.5 ± 1 fs [Fig. 5(a)]. The fit curves in Fig. 5(a) use again $\Delta=0$ and $\tau_C/T_2=3$, but $T_2=11.5\pm1.5$ fs. The oscillation frequency on the signal in Fig. 5(a) is 1000 cm^{-1} [Fig. 6(b)]. In water the observed oscillation frequency is 800 cm^{-1} [Fig. 6(c)]. The visible substructure in the absorption spectrum of crystal violet is known not to result from vibrations. In aqueous solution, especially for the high concentrations used in our experiment, the formation of dimers and higher oligomers of the dye molecule is met [41,56], which leads to the observed splitting [Fig. 3(c)]. In glycerol a different mechanism is operative in producing the splitting [Fig. 3(b)]. Different steric forms of the molecule (different rotamers [42,57]) as well as the influence of an asymmetric charge distribution in the dye cation [56] have been proposed. We excite the dye molecule on the short-wavelength edge, so that we excited predominantly one of the molecular species.

The line-shape analysis of the absorption shown in Figs. 3(b) and 3(c) indicates that we excited crystal violet above the 0-0 transition. If we use, however, the resulting $\Delta=280$ THz (corresponding to 1500 cm^{-1}) in the line-shape function (27), a very narrow coherence peak would result. So we conclude that $\Delta\approx0$ also for crystal violet, as a result of the excitation of a homogeneous subgroup in the absorption spectrum.

Unfortunately, a detailed analysis of the vibronic bands is not available for crystal violet, so we can compare our results only with those obtained for malachite green in a two-pulse photon echo experiment using pulses of 8 fs duration. Malachite green and crystal violet have a very similar chemical structure. Only one of the dimethylamino groups is replaced by a H atom for malachite green [cf. Fig. 3(c)]. Therefore, these dyes are expected to have similar optical properties. For example, resonance Raman experiments show that the frequencies of the strongest Raman active vibrations differ by ≤10 cm^{-1} for malachite green and crystal violet [56]. The transient absorption experiments of Migus *et al.* [58] give a spectral cross relaxation time of $\tau_X=0.45$ ps for malachite green, whereas $\tau_X=0.5$ ps for crystal violet [42]. Indeed, Becker *et al.* [13] observed an average exponential decay with a decay rate of 8 ± 2 fs for malachite green. This agrees favorably with our 6.5 ± 1 fs for crystal violet.

However, Becker *et al.* found a stronger periodic modulation of the dephasing kinetic and a modulation frequency of ~1700 cm^{-1}, which differs from the value found in our experiment with crystal violet. On the other hand, the spectrum is very broad in Fig. 6(b), so that it is difficult to compare the results in this respect. The higher modulation depth in the two-pulse photon echo experiment could be explained with the higher time resolution of ~12 fs. The broad autocorrelation time of 40 fs used in our experiment tends to average out these modulations. In addition, a slow dephasing process was observed also for delay times >60 fs in the experiment with malachite green. We were unable to resolve the dephasing kinetics in this region because the signal approached the noise level in our experiment.

So it can be concluded that the dephasing kinetics obtained here with an incoherent light technique for crystal violet are in close agreement with those found for malachite green in a two-pulse photon echo experiment using pulses of 8-fs duration. The analysis of our experiments is thus not basically limited to the Kubo model; the refined analysis of Becker *et al.* developed for malachite green can be applied to our results on crystal violet as well. Of course, the different tuning conditions with respect to the 0-0 transition of the relevant electronic transition should be considered. In addition the dephasing observed in a two-pulse photon echo experiment is not identical to the one obtained by forced light scattering [20,24], even for the same line-shape function. Nevertheless gross features are the same [e.g., decay with $\exp(-2|\tau|/T_2)$ for homogeneous broadening].

VI. CONCLUSIONS

Forced light scattering from a phase grating generated by broadband incoherent laser beams was introduced to study the dephasing of electronic transitions in large molecules. The method is a general tool to study the dephasing kinetics. The dynamic range of our experiments is improved compared to the frequently used self-diffraction techniques because the probing beam was not resonant to the absorption band of the dyes. Since a dephasing process is studied the long intensity correlation time of incoherent light does not influence the time resolution [59].

We find dephasing time parameters of $T_2 \approx 10$ fs and an intrinsic correlation time of $\tau_C \approx 30$ fs for solutions of crystal violet and heptamethine for excitation with a bandwidth of $\Delta\lambda_B = 13.8$ nm at $\lambda_B = 508$ nm. The T_2 time of the heptamethine dye is in good agreement with results of a resonance CARS line-shape analysis. Previous real-time two-pulse photon echo experiments with malachite green gave similar dephasing kinetics as described here for crystal violet. The bandwidth of the excited laser pulses is small compared to the overall width of the electronic absorption bands, leading to excitation of a subset of vibronic transitions. As a result, the phase relaxation behavior is close to that of a homogeneously broadened transition whereas the inhomogeneous broadening of the overall absorption band is of minor importance since spectral cross relaxation proceeds too slowly.

Our present technique using essentially nanosecond laser pulses can easily be extended to other spectral ranges. In particular, dephasing processes at different spectral positions within a broad absorption band can be studied. Such experiments are presently under way.

Note added. After this work was submitted we gained knowledge of a paper by Yang, Zhang, and Myers treating a coupling scheme similar to forced light scattering. The authors confine the work to the case of homogeneous broadening and "electronic" gratings, but allow for one-photon resonance of the probe beam.

ACKNOWLEDGMENT

This work was supported by the Deutsche Forschungsgemeinschaft.

[1] R. L. Fork, B. I. Greene, and C. V. Shank, Appl. Phys. Lett. **38**, 671 (1981).
[2] B. Nikolaus and D. Grishkowsky, Appl. Phys. Lett. **43**, 228 (1983).
[3] W. H. Knox, M. C. Downer, R. L. Fork, and C. V. Shank, Opt. Lett. **9**, 552 (1984).
[4] J. G. Fujimoto, A. M. Weiner, and E. P. Ippen, Appl. Phys. Lett. **44**, 832 (1984).
[5] W. H. Knox, R. L. Fork, M. C. Downer, R. H. Stolen, C. V. Shank, and J. A. Valdmanis, Appl. Phys. Lett. **46**, 1120 (1985).
[6] J. M. Evans, D. E. Spence, D. Burns, and W. Sibbett, Opt. Lett. **18**, 1074 (1993).
[7] V. Yanovsky, Y. Pang, F. Wise, and B. I. Minkov, Opt. Lett. **18**, 1541 (1993).
[8] B. Proctor and F. Wise, Appl. Phys. Lett. **62**, 470 (1993).
[9] A. M. Weiner, S. DeSilvestri, and E. P. Ippen, J. Opt. Soc. Am. B **2**, 654 (1985).
[10] A. M. Weiner and E. P. Ippen, Chem. Phys. Lett. **114**, 456 (1985).
[11] S. DeSilvestri, A. M. Weiner, J. G. Fujimoto, and E. P. Ippen, Chem. Phys. Lett. **12**, 195 (1984).
[12] A. M. Weiner and E. P. Ippen, Opt. Lett. **9**, 53 (1984).
[13] P. C. Becker, H. L. Fragnito, J. Y Bigot, C. H. Brito Cruz, R. L. Fork, and C. V. Shank, Phys. Rev. Lett. **63**, 505 (1989).
[14] E. T. J. Nibbering, D. A. Wiersma, and K. Duppen, Phys. Rev. Lett. **66**, 2464 (1991).
[15] E. T. J. Nibbering, D. A. Wiersma, and K. Duppen, Phys. Rev. Lett. **68**, 514 (1992).
[16] J. Y. Bigot, M. T. Portella, R. W. Schoenlein, C. J. Bardeen, A. Migus, and C. V. Shank, Phys. Rev. Lett. **66**, 1138 (1991).
[17] C. J. Bardeen and C. V. Shank, Chem. Phys. Lett. **203**, 535 (1993).
[18] T. Joo and A. C. Albrecht, Chem. Phys. **176**, 233 (1993).
[19] D. A. Wiersma, E. T. J. Nibbering, and, K. Duppen, in *Ultrafast Phenomena VIII*, edited by J. L. Martin, A. Migus, G. A. Mourou, and A. H. Zewail, Springer Series in Chemical Physics Vol. 55 (Springer, Berlin, 1993), pp. 611–615.
[20] B. D. Fainberg, Opt. Spectrosc. **55**, 669 (1983).
[21] R. F. Loring, Y. Jing Yan, and S. Mukamel, J. Chem. Phys. **87**, 5840 (1987).
[22] W. Vogel, D. G. Welsch, and B. Wilhelmi, Phys. Rev. A **37**, 3825 (1988).
[23] B. D. Fainberg, Opt. Spectrosc. **68**, 305 (1990).
[24] Y. Jing Yan and S. Mukamel, J. Chem. Phys. **94**, 179 (1991).
[25] S. Mukamel, Annu. Rev. Chem. Phys. **41**, 647 (1990).
[26] A. Asaka, H. Nakatsuka, M. Fujiwara, and M. Matsuoka, Phys. Rev. A **29**, 2286 (1984).
[27] R. Beach and S. R. Hartmann, Phys. Rev. Lett. **53**, 663 (1984).
[28] N. Morita and T. Yajima, Phys. Rev. A **30**, 2525 (1984).
[29] T. Yajima and N. Morita, in *Methods of Laser Spectroscopy*, edited by Y. Price, A. Ben-Reuven, and M. Rosenbluh (Plenum, New York, 1986), pp. 75–85.
[30] H. J. Eichler, P. Günter, and D. W. Pohl, *Laser-Induced Dynamic Gratings* (Springer, Berlin, 1986).
[31] N. Uchida and N. Niizeki, Proc. IEEE **61**, 1073 (1973).
[32] I. D. L. Albert, P. K. Das, and S. Ramasesha, J. Opt. Soc. Am. B **10**, 1365 (1993).
[33] D. A. Cremers and M. W. Windsor, Chem. Phys. Lett. **71**, 27 (1980).
[34] M. Fujiwara, R. Kuroda, and H. Nakatsuka, J. Opt. Soc. Am. B **2**, 1634 (1985).
[35] J. E. Golub and T. W. Mossberg, J. Opt. Soc. Am. B **3**, 554 (1986).
[36] K. Jarasiunas and J. Vaitkus, Phys. Status Solidi A **44**, 793 (1977).
[37] T. Elsaesser and W. Kaiser, Annu. Rev. Chem. Phys. **42**, 83 (1991).
[38] H. J. Eichler, F. Massmann, E. Biselli, K. Richter, M. Glotz, L. Konetzke, and X. Yang, Phys. Rev. B **36**, 3247 (1987).
[39] V. L. Vinetskii, N. V. Kukhtarev, S. G. Odulov, and M. S. Soskin, Usp. Fiz. Nauk **129**, 113 (1979) [Sov. Phys. Usp. **22**, 742 (1979)].
[40] J. Perina, *Coherence of Light* (Van Nostrand Reinhold, London, 1971); J. W. Goodman, *Statistical Optics* (Wiley, New York, 1985).
[41] F. Feichtmayr and J. Schlag, Ber. Bunsenges. **68**, 95 (1964).
[42] M. Ishikawa and Y. Maruyama, Chem. Phys. Lett. **219**, 416 (1994).

[43] Z. Q. Huang, Y. J. Xie, G. L. Huang, and H. S. Kwok, Opt. Lett. **15**, 501 (1990).
[44] F. Moshary, M. Arend, R. Friedberg, and S. R. Hartmann, Phys. Rev. A **46**, R33 (1992).
[45] N. V. Gruzdev, E. G. Silkis, V. D. Titov, and Yu. G. Vainer, J. Phys. (Paris) Colloq. **7**, C7-439 (1991).
[46] R. Zhang, T.-S. Yang, and A. B. Myers, Chem. Phys. Lett. **211**, 541 (1993).
[47] N. Wiener, Acta Math. **55**, 117 (1930).
[48] A. Khintchine, Math. Ann. **109**, 604 (1934).
[49] M. Born and E. Wolf, *Principles of Optics* (Pergamon, Oxford, 1991), p. 504.
[50] W. Koechner, *Solid State Laser Engineering* (Springer, Berlin, 1988), p. 454.
[51] R. Rentsch and B. Wilhelmi, J. Mol. Struct. **114**, 1 (1984).
[52] P. P. Kircheva, M. Pfeiffer, A. Lau, and W. Werncke, J. Raman Spectrosc. **20**, 183 (1989).
[53] A. Lau, M. Pfeiffer, W. Werncke, H. J. Weigmann, and K. Lenz, J. Raman Spectrosc. **19**, 353 (1988).
[54] W. Werncke, A. Lau, M. Pfeiffer, H. J. Weigemann, W. Freyer, J. T. Tschö, and M. B. Kim, Chem. Phys. **188**, 133 (1987).
[55] A. Lau, M. Pfeiffer, W. Werncke, H. J. Weigmann, and K. Lenz, J. Raman Spectrosc. **19**, 353 (1988).
[56] H. B. Lueck, D. C. Daniel, and J. L. McHale, J. Raman Spectrosc. **24**, 363 (1993).
[57] J. M. Grzybowski, S. E. Sugamori, D. F. Williams, and R. W. Yip, Chem. Phys. Lett. **65**, 456 (1979).
[58] A. Migus, A. Antonetti, J. Etchepare, D. Hulin, and A. Orszag, J. Opt. Soc. Am. B **2**, 584 (1985).
[59] T. Tokizaki, Y. Ishida, and T. Yajima, Opt. Commun. **71**, 355 (1989).
[60] T.-S. Yang, R. Zhang, and A. B. Myers, J. Chem. Phys. **100**, 8573 (1994).

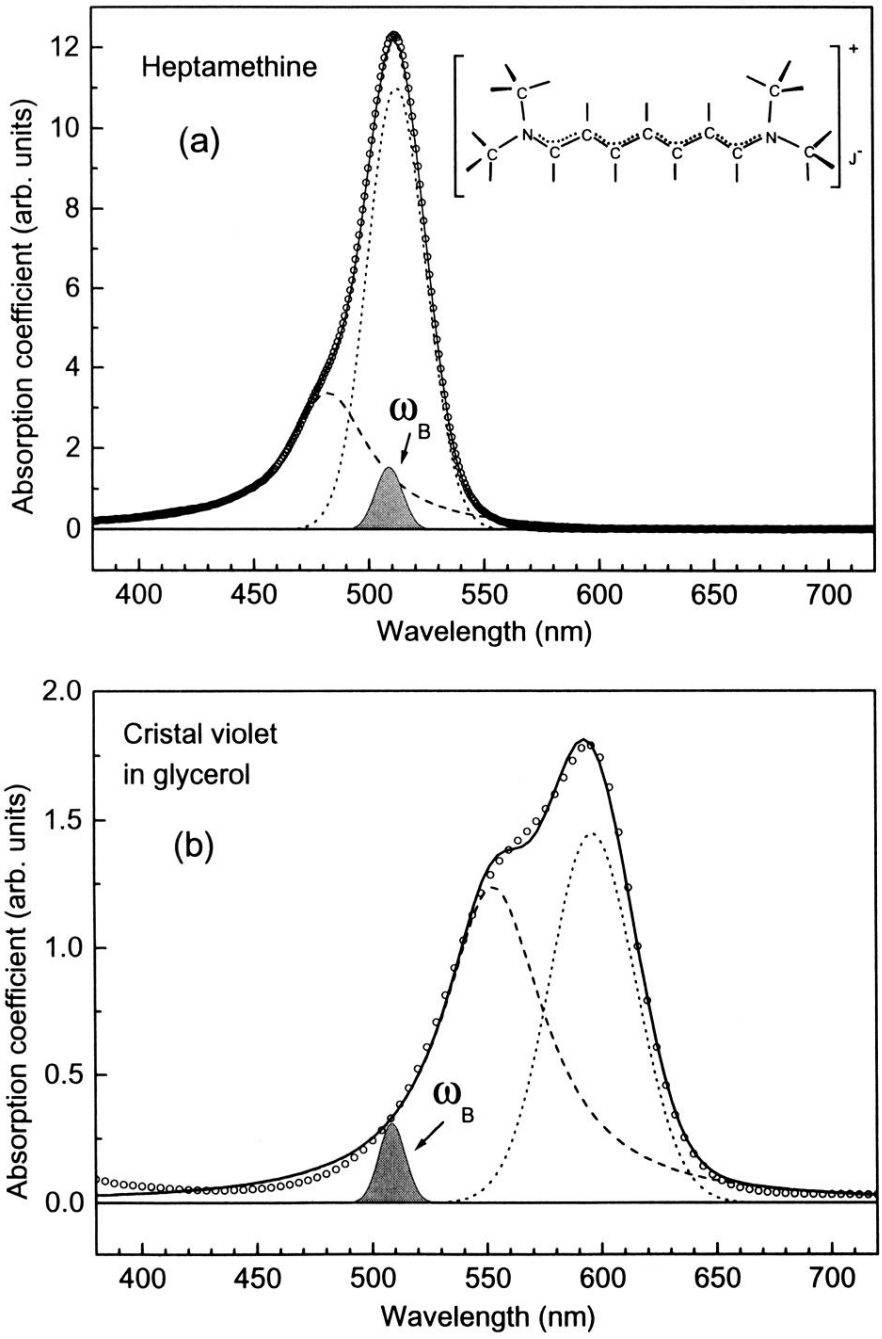

FIG. 3. Linear absorption spectra of the three dye solutions (always 1×10^{-3} mol/l). The heuristic fit (solid line) uses a Lorentzian line shape (broken line) for the short-wavelength side and a Gaussian (dotted line) for the long-wavelength side: (a) bis-(dimethylamino) heptamethine iodide in ethanol; (b) crystal violet chloride in glycerol; (c) crystal violet chloride in water. The broadband laser spectrum ω_B is shown as the hatched area.

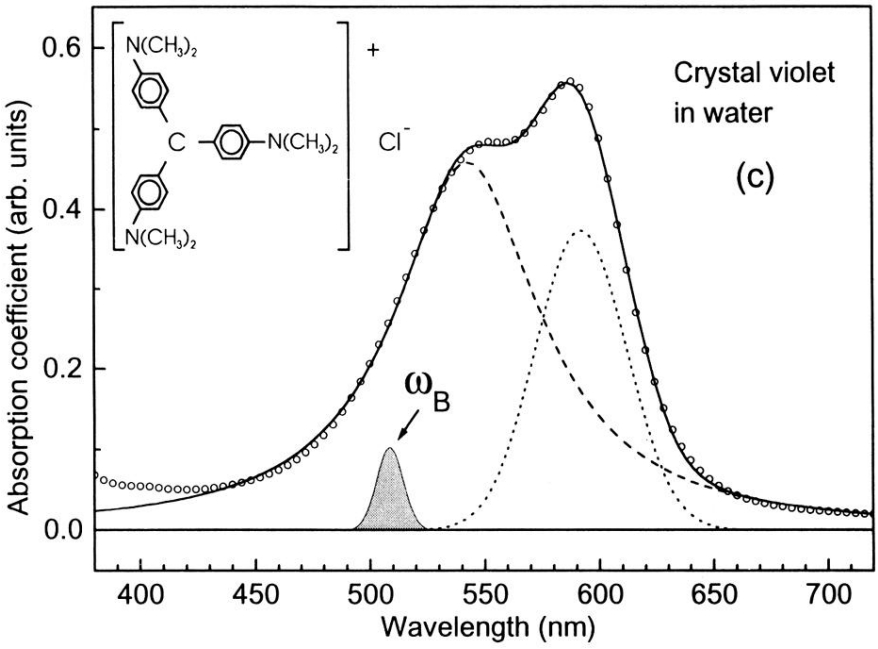

FIG. 3. (*Continued*).